
Research article

Forecasting mixture composition in the extractive distillation of n-hexane and ethyl acetate with n-methyl-2-pyrrolidone through ANN for a preliminary energy assessment

Daniel Chuquin-Vasco^{1,*}, Dennise Chicaiza-Sagal², Cristina Calderón-Tapia³, Nelson Chuquin-Vasco⁴, Juan Chuquin-Vasco⁴ and Lidia Castro-Cepeda⁵

¹ Escuela Superior Politécnica de Chimborazo (ESPOCH), Chemical Engineering Career, Safety, Environment and Engineering Research Group (GISAI), Riobamba, Chimborazo, Ecuador

² SOLMA, Advanced Mechanical Solutions, Mechanical Engineering and Construction Services, Quito, Pichincha, Ecuador

³ Escuela Superior Politécnica de Chimborazo (ESPOCH), Environmental Engineering Career, Riobamba, Chimborazo, Ecuador

⁴ Escuela Superior Politécnica de Chimborazo (ESPOCH), Mechanical Engineering Career, Safety, Environment and Engineering Research Group (GISAI), Riobamba, Chimborazo, Ecuador

⁵ SOLMA, Advanced Mechanical Solutions, Mechanical Engineering and Construction Services, Quito, Pichincha, Ecuador

* Correspondence: Email: daniel.chuquin@epoch.edu.ec; Tel: +593998163018.

Appendix A: Sensitivity analysis

The critical variables affecting the quality of n-hexane and ethyl acetate, the products of interest when modified in the extractive distillation and solvent recovery stages, were selected. Table A1 details the parameters that directly influence the purity of the components of interest.

Table A1. Variables used in the sensitivity analysis.

ANN	Column	Nomenclature	Parameter	Units
Inputs	Extractive (EDC)	T1-F	Feed flow inlet temperature	°C
		RR-EDC	EDC tower reflux ratio	
		FM1-F	Feed Stream Mass Flow	kg/h
	Recovery (ERC)	FM2-MU	Make-up stream mass flow	kg/h
		T-B1	Flow inlet temperature to ERC	°C
		RR-ERC	ERC tower reflux ratio	-
Outputs	Extractive (EDC)	FM-B1	Mass flow of the B1 stream (mixture)	kg/h
		X _{HE} -EDC	Mole fraction of n-hexane in the distillate of EDC	-
		X _{NMP} -EDC	Mole fraction of N-methyl-2 pyrrolidone in the bottom of EDC	-
	Recovery (ERC)	X _{EA} -ERC	Mole fraction of ethyl acetate in the distillate of ERC	-
		X _{NMP} -ERC	Mole fraction of N-methyl-2 pyrrolidone in the bottom of ERC	-

A.1. Results of the sensitivity analysis in the extractive distillation column

Four sensitivity analyses were performed on the most relevant design variables in the extractive distillation column (EDC): feed flow temperature, reflux ratio of the extractive distillation column, mass flow of the feed stream, and mass flow of the reflux stream. The parametric study was carried out using the tool available in ChemSep, applying different operating ranges based on the simulation performed in DWSIM. Table A2 details the sensitivity analyses performed in the EDC.

Table A2. Sensitivity analysis in the extractive distillation column.

Extractive distillation (EDC)				
# Analyses	Description	Independent variable	Dependent variable	
1	Analysis of the effect of the feed temperature to the EDC	T1-F	X _{HE}	X _{NMP1}
2	Analysis of the effect of the reflux ratio in the EDC	RR-ERC	X _{HE}	X _{NMP1}
3	Analysis of the effect of the mass flow of the feed	FM1-F	X _{HE}	X _{NMP1}
4	Analysis of the effect of the make-up mass flow	FM2-MU	X _{HE}	X _{NMP1}

A.1.1. Results of analysis #1

The ranges established for the analysis on the effect of the feed temperature in the EDC column were 20–150 °C, necessary to avoid overheating the outlet fluid of the recovered solvent in the heat exchanger (Figure A1). This design variable is used as an input for the ANN because there are significant changes in the fractions of n-hexane in the distillate, which decreases from 0.956 to 0.4 (a 58.3% decrease), and the NMP fraction in the bottom decreases from 0.556 to 0.478 (a 14.0% decrease) as the feed temperature increases. In both cases, as the inlet temperature rises, the molar fraction of the components decreases. The feed temperature directly impacts the column behavior, with higher temperatures reducing n-hexane recovery in the distillate and NMP purity at the bottom.

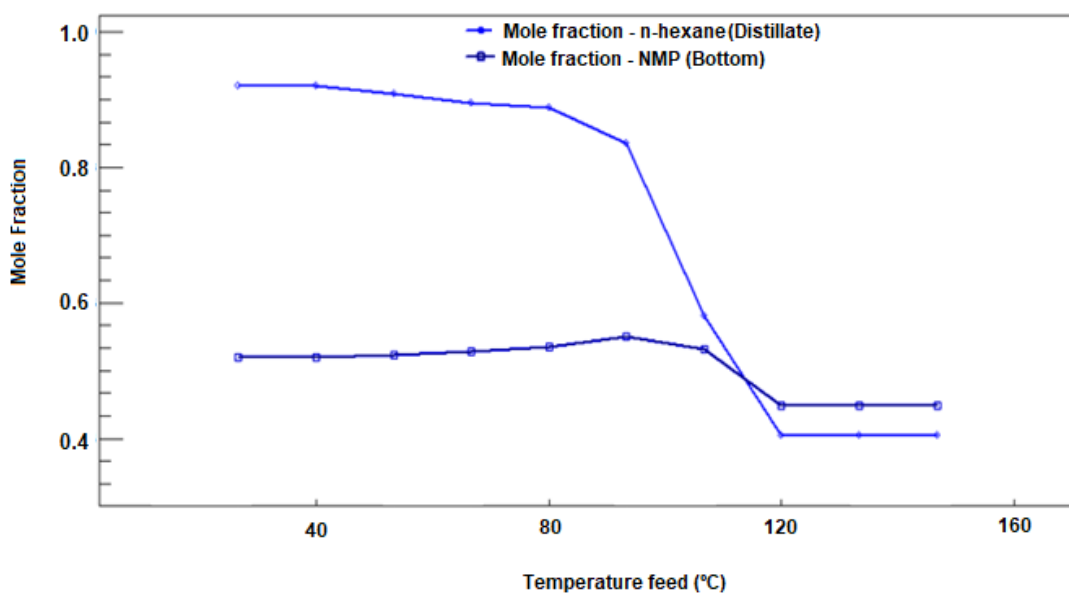


Figure A1. Molar fraction vs feed temperature to EDC.

A.1.2. Results of analysis #2

For the analysis of the reflux ratio of the EDC tower, a range of 0.7 to 2 was used, as observed in Figure A2. There is no significant increase in the fraction of n-hexane in the distillate or NMP in the bottom. The n-hexane practically remains constant with a fraction of 0.92 while the NMP changes from 0.51 to 0.49 (a 3.9% decrease). Therefore, as there are minimal changes in the key component fractions over the reflux ratio range analyzed, this variable is discarded as an input to the ANN model.

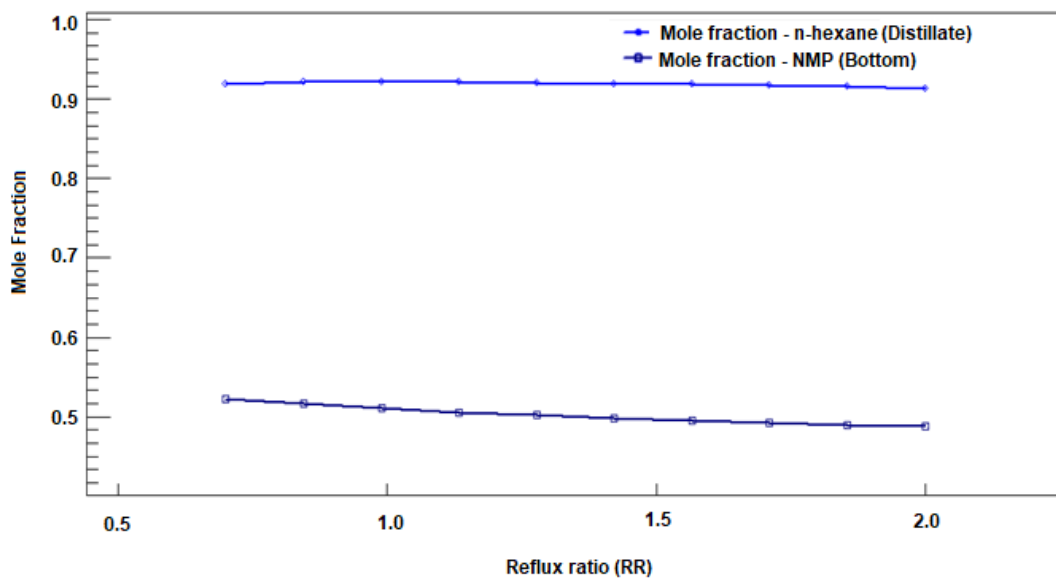


Figure A2. Molar fraction vs EDC reflux ratio.

A.1.3. Results of analysis #3

For this analysis, the mass flow rate of the feed was varied in a range from 8000 to 10,000 kg/h. In Figure A3, a significant increase in the molar fraction of NMP obtained at the bottom is shown, increasing from 0.37 to 0.69 (an 86.5% increase), while in the case of n-hexane, a decrease in its composition in the distillate is observed as the mass feed flow rate increases, with the fraction decreasing from 0.95 to 0.85 (a 10.5% decrease). Since there is a significant change in the concentrations with respect to the mass flow rate of the feed, this variable is taken as an input to the ANN model. The feed flow rate impacts the residence time and partial pressure of components in the column, directly altering the separation efficiency. Correlating this operational parameter will allow the optimization of purity and recovery targets.

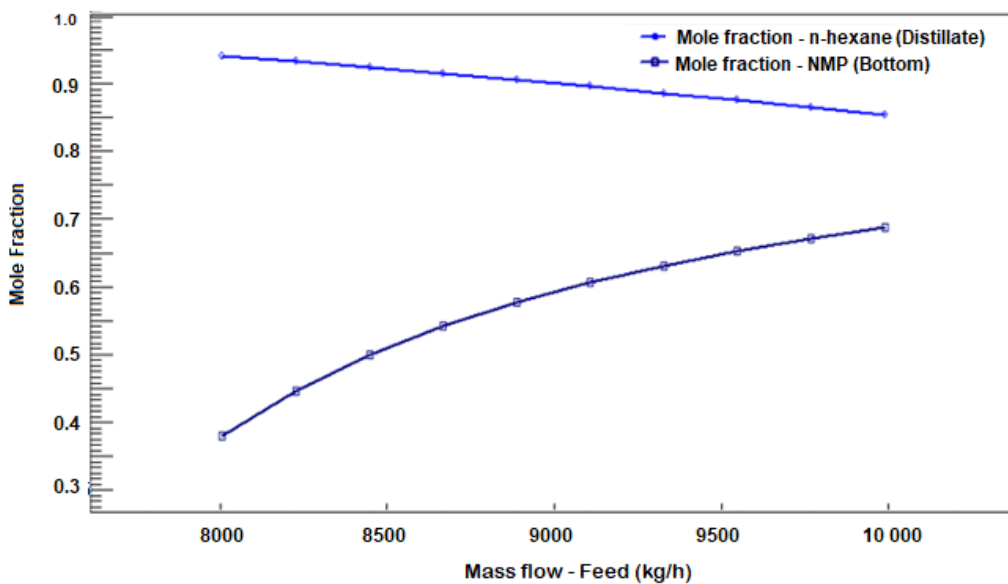


Figure A3. Molar fraction vs Mass flow-Feed.

A.1.4. Results of analysis #4

For this analysis, a range of 3 to 100 kg/h was used for the make-up flow rate entering the EDC. In Figure A4, a significant increase in n-hexane in the distillate is observed, with the molar fraction changing from 0.2 to 0.92 (a 360% increase), while the NMP fraction decreases from 1.0 to 0.3 (a 70% decrease). Since there are these significant changes, the make-up flow rate is chosen as an input to the ANN model. The make-up stream impacts the composition profile in the column, directly altering the recovery and purity. Correlating this operational parameter will allow the optimization of separation efficiency to achieve purity and recovery targets.

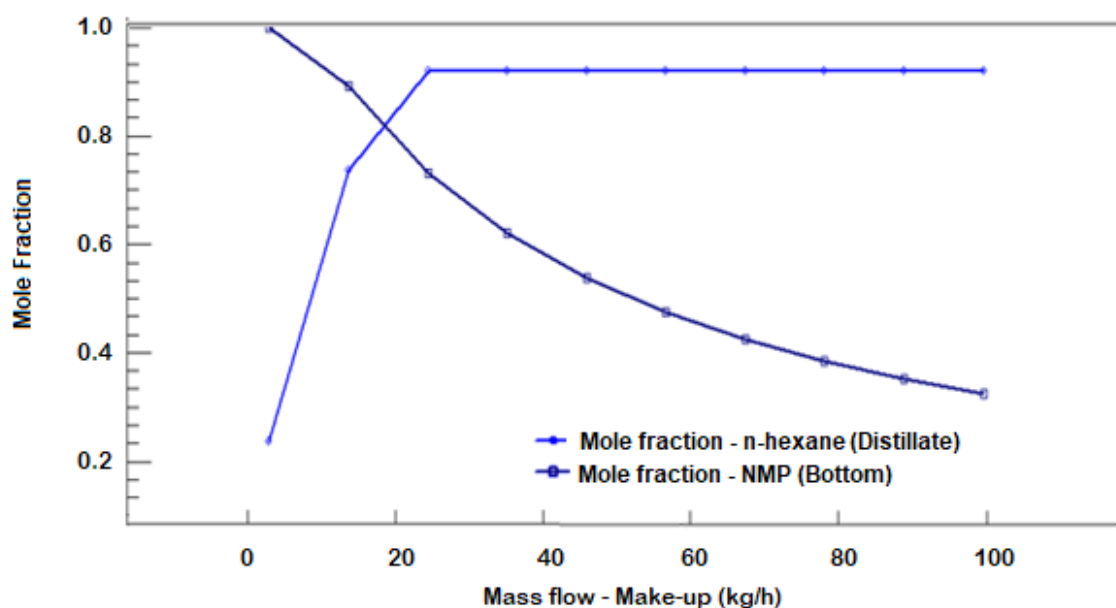


Figure A4. Molar fraction vs Mass flow—Make-up.

A.2. Results of the sensitivity analysis in the recovery distillation column

Three sensitivity analyses were performed on the most relevant design variables in the recovery distillation column (ERC): feed flow temperature, reflux ratio of the recovery column, and mass flow rate of stream B1 (Table A3). The parametric study was carried out using the tool available in ChemSep, applying different operating ranges based on the simulation performed in DWSIM. The key parameters were identified that have the most influence on purity and recovery of solvent and product. Understanding the relationships between inputs and outputs will allow developing an optimized model for the separation system.

Table A3. Sensitivity analysis in the recovery distillation column.

Recovery distillation (ERC)			
# Analyses	Description	Independent variable	Dependent variable
5	Analysis of the effect of B1 feed temperature to the recovery extractive column	T-B1	X_AE
			X_NMP2
6	Analysis of the effect of the reflux ratio in the ERC	RR-ERC	X_AE
			X_NMP2
7	Analysis of the effect of B1 feed mass flow rate	FM-B1	X_AE
			X_NMP2

A.2.1. Results of analysis #5

For the analysis of the B1 feed stream temperature to the ERC, a range of 100 to 120 °C was used. The results shown in Figure A5 demonstrate that the molar fraction of ethyl acetate in the ERC distillate and NMP in the ERC bottom remains constant throughout the analysis. Therefore, this parameter is discarded as a design variable for the ANN model since it has minimal effect on the component separations under the conditions evaluated.

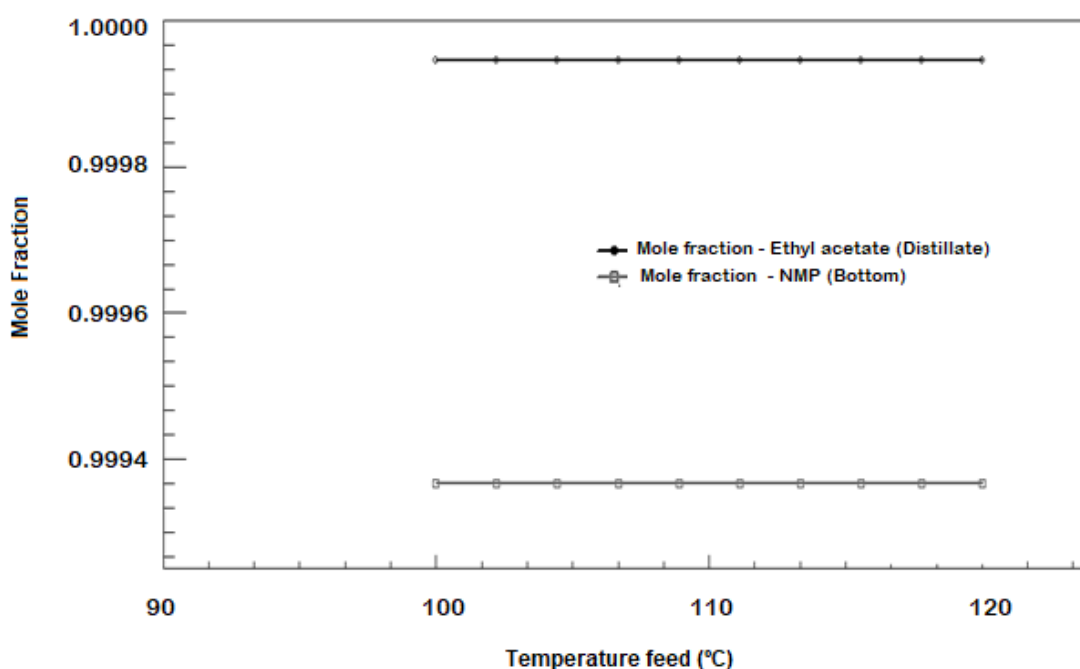


Figure A5. Molar fraction vs feed temperature to ERC.

A.2.2. Results of analysis #6

For the analysis of the reflux ratio in the ERC, a range of 0.8 to 2.0 was employed. Figure A6 illustrates the observed variation in the increase of molar fractions for the targeted components. The molar fraction of Ethyl Acetate in the distillate changes from 0.83 to 1 (a 20% increase), while NMP changes from 0.91 to 0.98 (a 7.69% increase). Consequently, the reflux ratio is selected as the input variable for the development of the ANN.

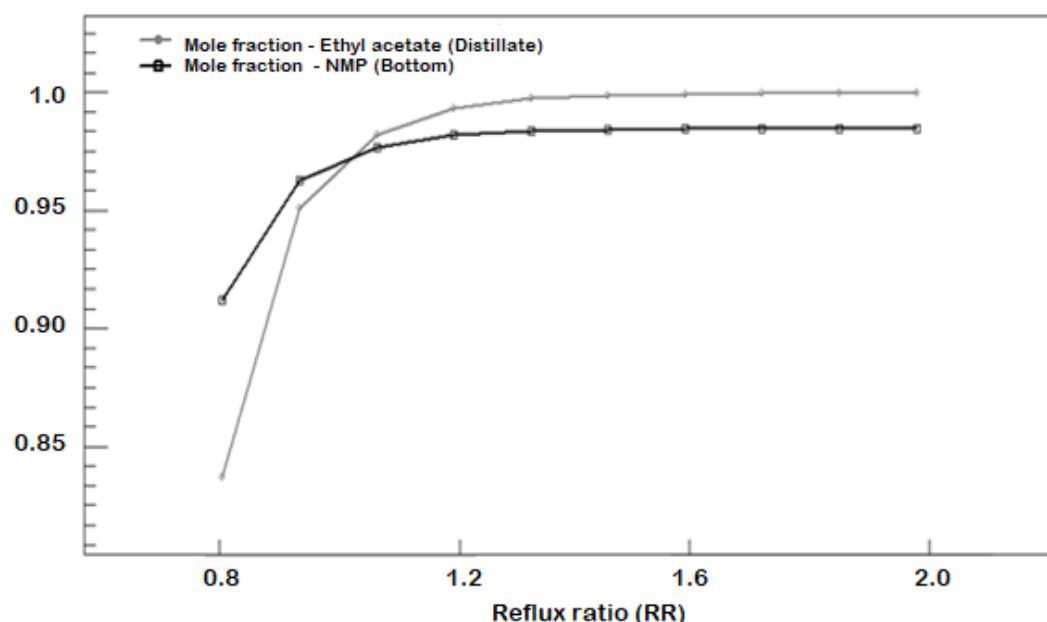


Figure A6. Molar fraction vs ERC reflux ratio.

A.2.3. Results of analysis #7

The feed flow rate to the ERC was ultimately varied within the range of 10,000 to 20,000 kg/h. As depicted in Figure A7, it is evident that the molar fractions of the targeted compounds remain constant across this range. Consequently, this parameter is not chosen as an input for the ANN due to its lack of significant impact on the observed variations in the molar fractions of the compounds of interest.

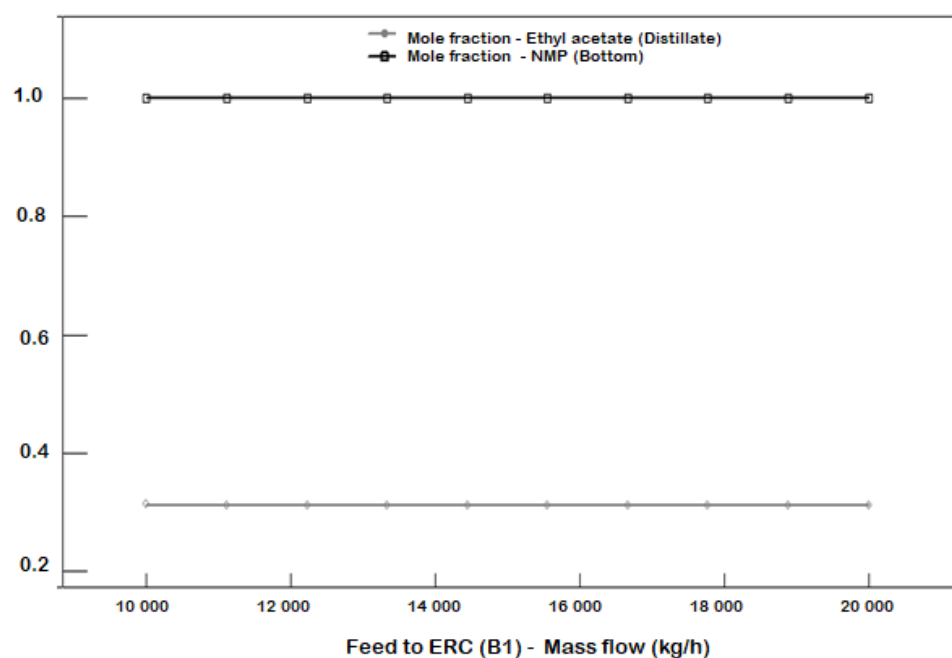


Figure A7. Molar fraction vs Feed mass flow rate to ERC.

Appendix B: Database generated for simulation parameters, training, and validation of the ANN

The database was established by a random number considering restrictions of mass flow, temperature and reflux ratio. Our objective, in addition to simulating and predicting the compositions at the outlet of the Extractive Distillation (EDC) and Recovery Column (ERC).

Data pair	Inputs				Outputs			
	Feed flow inlet (T1-F)	Feed stream mass flow (FM1-F)	Make-up stream mass flow (FM2-MU)	ERC tower reflux ratio (RR-ERC)	Distillate of EDC (XHE-EDC)	Bottom of EDC (XNMP-EDC)	Distillate of ERC (XEA-ERC)	Bottom of ERC (XNMP-ERC)
1	50	0.87	9706	69	0.8110	0.7576	0.9755	0.9999
2	78	1.2	9518	67	0.9487	0.6888	0.9830	1.0000
3	130	1.65	8278	16	0.9960	0.6710	0.8725	1.0000
4	97	1.88	9158	17	0.9948	0.6187	0.7675	1.0000
5	107	1.1	9816	29	0.9137	0.6965	0.9923	1.0000
6	27	0.89	9935	22	1.0000	0.4881	0.4925	1.0000
7	106	1.54	8409	50	0.9954	0.6792	0.9076	1.0000
8	49	1.38	8973	83	0.9929	0.6801	0.9567	1.0000

9	22	1.55	9766	5	1.0000	0.4760	0.4632	1.0000
10	54	1.96	9022	62	0.9954	0.6183	0.7451	1.0000
11	40	1.9	9478	73	0.9943	0.6082	0.7470	1.0000
12	89	1.42	8511	45	0.9944	0.6904	0.9670	1.0000
13	145	1.6	8344	83	0.9959	0.6757	0.8767	1.0000
14	22	0.9	9446	54	1.0000	0.5047	0.4967	1.0000
15	118	1.5	8037	79	0.9961	0.6990	0.9404	1.0000
16	74	1.1	9023	94	0.8913	0.7260	0.9719	1.0000
17	107	1.8	8307	89	0.9966	0.6573	0.8043	1.0000
18	101	0.8	8959	22	0.7623	0.7893	0.9895	0.9781
19	106	1.6	8690	48	0.9951	0.6621	0.8690	1.0000
20	116	1	9240	26	0.8549	0.7387	0.9915	1.0000
21	75	1.5	9922	69	0.9910	0.6323	0.8612	1.0000
22	46	1.4	9960	25	0.9896	0.6424	0.9131	1.0000
23	28	1.7	9025	67	1.0000	0.4986	0.4618	1.0000
24	101	1.5	8128	9	0.9957	0.6937	0.9525	1.0000
25	140	1.44	8480	22	0.9945	0.6883	0.9627	1.0000
26	93	1.67	9715	99	0.9946	0.6214	0.8009	1.0000
27	27	1.72	9281	62	1.0000	0.4898	0.4591	1.0000
28	71	1.02	9388	92	0.8676	0.7302	0.9719	1.0000
29	61	1.67	9781	19	0.9924	0.6171	0.8108	1.0000
30	88	1.59	9032	18	0.9941	0.6503	0.8652	1.0000
31	36	1	8757	75	0.8411	0.7578	0.9734	1.0000
32	107	1.2	9808	44	0.9570	0.6784	0.9893	1.0000
33	23	1.8	8876	22	1.0000	0.5005	0.4624	1.0000
34	41	1.6	9038	59	0.9941	0.6501	0.8535	1.0000
35	43	2	8904	41	0.9957	0.6187	0.7417	1.0000
36	80	0.87	8330	15	0.7741	0.7959	0.9927	0.9839
37	87	1.38	8244	18	0.9819	0.7055	0.9950	1.0000
38	44	1.9	9299	50	0.9945	0.6134	0.7543	1.0000
39	108	0.82	9611	34	0.7871	0.7756	0.9864	0.9995
40	82	1.9	8089	61	0.9971	0.6561	0.7871	1.0000
41	32	1	9948	88	1.0000	0.4860	0.4818	1.0000
42	50	1.3	9061	78	0.9774	0.6886	0.9803	1.0000
43	68	1.1	8960	56	0.9774	0.7274	0.9828	1.0000
44	63	1.52	8205	71	0.9958	0.6898	0.9229	1.0000
45	81	0.92	9602	73	0.8301	0.7472	0.9755	1.0000
46	35	1.18	8905	69	0.9215	0.7142	0.9803	1.0000
47	59	1.48	8005	61	0.9960	0.7023	0.9578	1.0000
48	98	1.09	8044	7	0.8554	0.7639	0.9974	1.0000
49	76	0.8	8940	29	0.7618	0.7900	0.9861	0.9779
50	65	1.9	9884	43	0.9938	0.5945	0.7417	1.0000
51	107	0.9	9205	57	0.8113	0.7668	0.9786	0.9999
52	102	1.2	8686	96	0.9228	0.7193	0.9722	1.0000
53	124	1.5	8624	18	0.9946	0.6753	0.9237	1.0000
54	148	2	8047	5	0.9972	0.6484	0.7713	1.0000

55	63	1.9	8373	61	0.9966	0.6456	0.7780	1.0000
56	103	1.8	9783	88	0.9931	0.6071	0.7630	1.0000
57	20	1.3	9852	69	1.0000	0.4804	0.4687	1.0000
58	53	1.6	9820	96	0.9923	0.6251	0.8219	1.0000
59	128	2	8910	48	0.9957	0.6187	0.7406	1.0000
60	36	1.5	9175	96	0.9933	0.6577	0.8836	1.0000
61	24	1.9	8398	95	1.0000	0.5174	0.4599	1.0000
62	77	0.9	8059	50	0.7781	0.8019	0.9749	0.9877
63	89	1.3	8292	13	0.9507	0.7155	0.9964	1.0000
64	23	1.5	9267	83	1.0000	0.4950	0.4656	1.0000
65	39	1.71	8262	50	0.9963	0.6664	0.8433	1.0000
66	93	1.84	8068	46	0.9970	0.6616	0.8080	1.0000
67	35	0.96	8507	55	0.8168	0.7771	0.9781	0.9999
68	113	1.6	9742	13	0.9920	0.6254	0.8371	1.0000
69	55	1.62	9049	29	0.9942	0.6468	0.8507	1.0000
70	84	0.9	8429	16	0.7895	0.7943	0.9928	0.9978
71	22	1.5	8677	19	1.0000	0.5131	0.4756	1.0000
72	130	1.2	8905	79	0.9300	0.7108	0.9779	1.0000
73	77	1.1	8448	94	0.8732	0.7477	0.9687	1.0000
74	107	1.3	8424	34	0.9555	0.7110	0.9903	1.0000
75	50	0.8	9819	57	0.7833	0.7753	0.9775	0.9995
76	68	1.78	8768	58	0.9955	0.6417	0.8006	1.0000
77	95	1.88	9769	55	0.9934	0.6000	0.7475	1.0000
78	102	1.29	9698	24	0.9886	0.6668	0.9876	1.0000
79	87	1.62	9393	89	0.9935	0.6367	0.8289	1.0000
80	31	1.71	8308	75	0.9963	0.6654	0.8368	1.0000
81	55	0.9	8711	18	0.7977	0.7845	0.9924	0.9995
82	64	1.22	9587	67	0.9594	0.6830	0.9835	1.0000
83	109	1.18	8615	88	0.9121	0.7255	0.9737	1.0000
84	99	1.26	9734	37	0.9810	0.6706	0.9912	1.0000
85	98	0.87	9857	38	0.8146	0.7516	0.9867	0.9999
86	81	0.86	9763	86	0.8146	0.7590	0.9694	0.9999
87	69	1.43	9402	91	0.9921	0.6586	0.9085	1.0000
88	109	2	9146	80	0.9953	0.6117	0.7309	1.0000
89	81	1.4	9746	16	0.9898	0.6491	0.9237	1.0000
90	141	1.8	8921	17	0.9951	0.6335	0.7964	1.0000
91	28	1.9	8341	14	1.0000	0.5171	0.4652	1.0000
92	114	0.8	9999	52	0.7873	0.7690	0.9802	0.9997
93	60	1.21	9604	14	0.9555	0.6828	0.9965	1.0000
94	22	1.58	8500	32	1.0000	0.5180	0.4736	1.0000
95	54	0.99	8780	69	0.8375	0.7592	0.9753	1.0000
96	80	1.5	9151	85	0.9934	0.6583	0.8866	1.0000
97	116	0.84	9249	42	0.7868	0.7825	0.9826	0.9993
98	65	0.93	8886	43	0.8153	0.7701	0.9834	0.9999
99	90	1.4	8513	40	0.9943	0.6930	0.9801	1.0000
100	90	1	8765	47	0.8413	0.7569	0.9832	1.0000

101	30	1.3	8532	46	0.9594	0.7072	0.9872	1.0000
102	120	1.7	8547	6	0.9956	0.6558	0.8440	1.0000
103	104	1.3	9088	40	0.9783	0.6867	0.9899	1.0000
104	55	1.4	8772	86	0.9920	0.6846	0.9547	1.0000
105	95	0.87	9456	96	0.8049	0.7672	0.9645	0.9999
106	120	1.38	8171	11	0.9791	0.7081	0.9969	1.0000
107	85	1.66	9132	79	0.9944	0.6411	0.8247	1.0000
108	60	1.93	9546	27	0.9940	0.6024	0.7443	1.0000
109	50	1.84	8973	9	0.9951	0.6280	0.7845	1.0000
110	61	0.81	9832	44	0.7879	0.7713	0.9829	0.9996
111	106	1.29	8266	73	0.9456	0.7195	0.9787	1.0000
112	110	1.66	9363	62	0.9937	0.6329	0.8201	1.0000
113	68	1.24	9850	48	0.9756	0.6703	0.9887	1.0000
114	109	0.82	9301	51	0.7795	0.7866	0.9785	0.9985
115	85	1.82	9606	88	0.9921	0.6110	0.7619	1.0000
116	31	0.94	8798	55	0.8170	0.7710	0.9788	0.9999
117	46	1.02	8662	84	0.8466	0.7569	0.9705	1.0000
118	20	1.43	9361	73	0.9999	0.4931	0.4680	1.0000
119	102	1.24	8798	41	0.9434	0.7069	0.9886	1.0000
120	100	0.97	8919	86	0.8332	0.7593	0.9694	1.0000
121	150	1.09	9138	49	0.8904	0.7228	0.9853	1.0000
122	28	1.73	9541	40	1.0000	0.4808	0.4576	1.0000
123	139	0.99	8243	18	0.8210	0.7792	0.9926	0.9999
124	62	1.86	8264	14	0.9964	0.6517	0.8007	1.0000
125	116	1.3	9361	95	0.9870	0.6785	0.9772	1.0000
126	50	0.8	9300	23	0.7709	0.7884	0.9894	0.9928
127	100	1.4	8060	79	0.9829	0.7112	0.9779	1.0000
128	43	1.9	9954	80	0.9931	0.5934	0.7358	1.0000
129	92	1.8	9457	7	0.9931	0.6153	0.7823	1.0000
130	96	0.86	8560	9	0.7766	0.7940	0.9960	0.9892
131	39	1.61	9944	46	0.9861	0.6188	0.8223	1.0000
132	86	1.08	8740	57	0.8742	0.7399	0.9814	1.0000
133	115	1.82	9776	92	0.9933	0.6057	0.7574	1.0000
134	40	1.07	8490	27	0.8621	0.7509	0.9906	1.0000
135	110	1.77	9946	89	0.9927	0.6046	0.7671	1.0000
136	139	1.42	8197	60	0.9927	0.7027	0.9817	1.0000
137	104	1.13	9928	48	0.9298	0.6873	0.9878	1.0000
138	93	1.44	8631	23	0.9942	0.6828	0.9541	1.0000
139	73	0.93	9976	22	0.8436	0.7303	0.9931	1.0000
140	108	1.52	9010	74	0.9939	0.6605	0.8853	1.0000
141	23	1.64	8049	97	1.0000	0.5352	0.4728	1.0000
142	136	1.07	8577	31	0.8649	0.7477	0.9894	1.0000
143	50	1.17	8077	43	0.8893	0.7473	0.9854	1.0000
144	36	1.13	9131	16	0.9073	0.7142	0.9953	1.0000
145	101	1.29	8277	90	0.9460	0.7195	0.9739	1.0000
146	89	1.58	9095	83	0.9941	0.6509	0.8551	1.0000

147	138	1.4	8718	89	0.9939	0.6866	0.9569	1.0000
148	46	1.56	8567	75	0.9953	0.6717	0.8859	1.0000
149	108	1.05	9292	27	0.8778	0.7253	0.9917	1.0000
150	107	0.84	9912	52	0.8028	0.7592	0.9812	0.9999
151	57	1.1	8358	69	0.8702	0.7506	0.9764	1.0000
152	67	1.14	9459	55	0.9212	0.7015	0.9851	1.0000
153	26	0.9	8054	38	1.0000	0.5563	0.5226	1.0000
154	66	1.5	9176	31	0.9932	0.6560	0.8959	1.0000
155	42	1.3	8903	93	0.9722	0.6946	0.9760	1.0000
156	108	1.2	9891	19	0.9593	0.6750	0.9954	1.0000
157	49	1.3	8506	58	0.9584	0.7084	0.9838	1.0000
158	22	0.81	9042	57	1.0000	0.5226	0.5102	1.0000
159	42	1.13	9427	9	0.9160	0.7035	0.9975	1.0000
160	45	0.89	8652	45	0.7918	0.7900	0.9805	0.9992
161	109	0.85	9336	92	0.7933	0.7774	0.9640	0.9997
162	89	1.25	8009	66	0.9195	0.7361	0.9790	1.0000
163	62	1.82	8184	86	0.9968	0.6600	0.8029	1.0000
164	135	0.92	8403	89	0.7970	0.7924	0.9619	0.9995
165	91	1.69	8742	49	0.9948	0.6509	0.8326	1.0000
166	135	1.92	8998	42	0.9953	0.6216	0.7580	1.0000
167	42	1.77	8215	48	0.9966	0.6624	0.8246	1.0000
168	71	1.59	8388	63	0.9957	0.6746	0.8831	1.0000
169	50	0.9	9081	63	0.8080	0.7715	0.9758	0.9999
170	24	1	9853	95	0.9998	0.4892	0.4825	1.0000
171	117	1.9	9373	21	0.9944	0.6101	0.7563	1.0000
172	22	1.2	8391	53	1.0000	0.5323	0.4925	1.0000
173	98	1.7	8421	88	0.9961	0.6625	0.8337	1.0000
174	112	2	9636	16	0.9939	0.5941	0.7282	1.0000
175	30	1.2	8818	3	1.0000	0.5152	0.4894	1.0000
176	75	1.69	9697	21	0.9928	0.6179	0.8065	1.0000
177	103	1.43	9200	61	0.9925	0.6648	0.9231	1.0000
178	108	1.87	9864	33	0.9932	0.5972	0.7505	1.0000
179	101	1.29	8458	30	0.9526	0.7112	0.9914	1.0000
180	83	0.9	8302	33	0.7856	0.7982	0.9846	0.9960
181	54	1.18	9689	58	0.9450	0.6863	0.9854	1.0000
182	34	1.81	8422	76	0.9964	0.6519	0.7997	1.0000
183	22	0.82	8451	21	1.0000	0.5435	0.4741	1.0000
184	113	1.99	8459	22	0.9965	0.6345	0.7586	1.0000
185	96	1.19	9477	41	0.9432	0.6913	0.9894	1.0000
186	97	1.8	9233	4	0.9943	0.6226	0.7890	1.0000
187	109	1.3	8336	51	0.9523	0.7147	0.9853	1.0000
188	35	1.53	9769	12	0.9915	0.6322	0.8635	1.0000
189	30	0.8	9167	57	0.9999	0.5185	0.5089	1.0000
190	50	1.92	9692	58	0.9938	0.5994	0.7394	1.0000
191	132	1.69	8867	61	1.0000	0.6468	0.8261	1.0000
192	64	1.78	9178	85	0.9951	0.6284	0.7843	1.0000

193	108	0.99	9673	19	0.8622	0.7255	0.9942	1.0000
194	40	1.87	9909	62	0.9928	0.5966	0.7459	1.0000
195	52	1.19	9625	17	0.9475	0.6856	0.9957	1.0000
196	43	0.84	8596	45	0.7693	0.7958	0.9784	0.9845
197	46	1.25	9735	16	0.9767	0.6717	0.9962	1.0000
198	29	1.02	9681	9	0.8754	0.7179	0.9973	1.0000
199	106	1.32	8651	98	0.9719	0.7009	0.9740	1.0000
200	47	1.75	8009	76	0.9969	0.6728	0.8342	1.0000
201	71	1.28	9523	75	0.9834	0.6755	0.9821	1.0000
202	33	1.95	9192	94	0.9952	0.6142	0.7391	1.0000
203	34	0.97	8012	89	0.8052	0.7949	0.9614	0.9996
204	26	1.68	8722	61	1.0000	0.5090	0.4658	1.0000
205	32	0.84	9399	95	1.0000	0.5098	0.4995	1.0000
206	95	1.99	9400	63	0.9947	0.6036	0.7296	1.0000
207	38	1.74	9292	81	0.9943	0.6281	0.7936	1.0000
208	79	1.57	8247	76	0.9960	0.6825	0.8957	1.0000
209	55	1.31	9935	14	0.9881	0.6556	0.9656	1.0000
210	110	1.32	9325	19	0.9906	0.6748	0.9894	1.0000
211	28	1.07	9639	58	1.0000	0.4928	0.4829	1.0000
212	65	0.99	9723	92	0.8635	0.7255	0.9725	1.0000
213	24	1.63	9092	22	1.0000	0.4964	0.4659	1.0000
214	97	1.89	8812	30	0.9956	0.6300	0.7725	1.0000
215	116	1.73	9152	95	0.9946	0.6341	0.7985	1.0000
216	135	1.48	8560	84	0.9949	0.6818	0.9224	1.0000
217	69	1.07	8339	49	0.8572	0.7573	0.9825	1.0000
218	89	0.92	8439	25	0.7981	0.7895	0.9891	0.9993
219	92	1.65	9303	79	0.9932	0.6364	0.8227	1.0000
220	27	1.3	9200	100	1.0000	0.5022	0.4738	1.0000
221	53	1.5	8593	95	0.9950	0.6784	0.9085	1.0000
222	103	1.2	8405	30	0.9133	0.7285	0.9907	1.0000
223	57	1.9	8570	36	0.9962	0.6379	0.7760	1.0000
224	119	1.81	8970	45	0.9946	0.6317	0.7876	1.0000
225	45	1.18	8927	100	0.9222	0.7141	0.9718	1.0000
226	45	1.73	9400	54	0.9939	0.6247	0.7976	1.0000
227	114	1.47	9919	98	0.9909	0.6368	0.8693	1.0000
228	55	2	8778	34	0.9959	0.6228	0.7459	1.0000
229	134	1.45	8748	17	0.9939	0.6770	0.9437	1.0000
230	27	1.1	9181	74	1.0000	0.5076	0.4860	1.0000
231	56	1.36	9467	33	0.9908	0.6644	0.9547	1.0000
232	55	1.73	9006	40	0.9948	0.6376	0.8117	1.0000
233	124	1.17	8190	95	0.8933	0.7439	0.9689	1.0000
234	94	1.13	8623	61	0.8914	0.7341	0.9807	1.0000
235	77	1.48	8280	19	0.9953	0.6906	0.9522	1.0000
236	36	0.89	9618	83	0.8175	0.7552	0.9711	0.9999
237	67	1.35	8256	60	0.9700	0.7104	0.9831	1.0000
238	115	1.43	9236	24	0.9924	0.6625	0.9291	1.0000

239	76	1.34	9511	84	0.9907	0.6671	0.9535	1.0000
240	60	1.05	8436	27	0.8520	0.7575	0.9902	1.0000
241	80	1.83	8192	29	0.9967	0.6574	0.8096	1.0000
242	47	1.72	8021	44	0.9968	0.6744	0.8508	1.0000
243	108	1.92	9046	6	0.9951	0.6190	0.7619	1.0000
244	28	1.32	9531	88	1.0000	0.4905	0.4701	1.0000
245	94	1.72	9692	10	0.9929	0.6149	0.7988	1.0000
246	70	0.93	8305	16	0.7981	0.7918	0.9929	0.9991
247	48	0.81	9169	42	0.7719	0.7909	0.9813	0.9938
248	150	1.61	8969	42	0.9930	0.6510	0.8552	1.0000
249	107	1.99	8577	29	0.9963	0.6305	0.7543	1.0000
250	118	1.82	8928	89	0.9954	0.6335	0.7793	1.0000



AIMS Press

© 2024 the Author(s), licensee AIMS Press. This is an open access article distributed under the terms of the Creative Commons Attribution License (<http://creativecommons.org/licenses/by/4.0>)